Model of the oculomotor system based on adaptive internal models ⋆

Mireille E. Broucke *

* *Dept. of Electrical and Computer Engineering, University of Toronto, Canada (e-mail: broucke@control.utoronto.ca).*

Abstract: We propose a new model of the oculomotor system, particularly, the slow eye movement systems. We show that the system can be best understood as an application of adaptive internal models. The outcome is a simple model that includes the interactions between the brainstem and the cerebellum and that accounts for behaviors in a number of oculomotor experiments. Our model suggests that a possible role of the cerebellum is to embody adaptive internal models of persistent, exogenous disturbance signals acting on the body and observable through the sensory error signals it receives.

Keywords: Adaptive internal models, oculomotor system, cerebellum

1. INTRODUCTION

The purpose of this paper is to derive a unified model of the oculomotor system based on adaptive internal models [Nikiforov, 1996, 1997, 1998, Serrani and Isidori, 2000, Serrani et.al., 2001, Marino and Tomei, 2011, 2013]. Control-theoretic models of the oculomotor system have a long history [Robinson, 1981], and recent models include [Zhang and Wakamatsu, 2001, Pola, 2002, Glasauer, 2003]. Unfortunately, existing models are still limited in the behaviors they capture. This may be partly due to the fact that a suitable computational model of the cerebellum, an important component of the oculomotor system, is not available. Since the 1990's, neuroscientists have explored the idea that the cerebellum may embody internal models of the systems it controls [Gomi and Kawato, 1992, Kawato and Gomi, 1992, Wolpert et.al., 1998, Porrill, et.al., 2004, Dean and Porrill, 2008].

The last 25 years of developments in control theory have meanwhile positioned the internal model principle [Francis and Wonham, 1975, 1976] to be relevant in biological problems: a biological system must be able to reject incoming disturbance and reference signals using only sensory error measurements with limited (or no) knowledge of the plant model. We exploit these developments in control theory to present a unified control-theoretic model of the oculomotor system (specifically the slow eye movement systems) that incorporates a computational model of the cerebellum.

The premise of our model, that a possible role of the cerebellum is to provide internal models of persistent, exogenous error signals acting on the body, has been suggested for the oculomotor system in [Cerminara et.al., 2009, Churchland et.al., 2003, Lisberger, 2009]. Experimental evidence supporting this idea comes in four forms. First, there is the so-called predictive capability of the smooth pursuit system - to track moving targets with zero steady-state error [Bahill and McDonald, 1983, Deno et.al, 1995], despite up to 100ms of processing delay of the retinal error signal. Second, it has been shown experimentally that exogenous signals that can be modeled by low-order linear exosystems are easily tracked, while unpredictable signals are not [Bahill, 1983, Collewijn and Tamminga, 1984, Deno et.al, 1995]. Third, in an experiment called *target blanking*, a moving target is temporarily occluded, yet the eye continues to move [Cerminara et.al., 2009, Churchland et.al., 2003]; researchers postulate the brain has an internal model of the motion of the target. Fourth, in an experiment called the *error clamp*, the retinal error is artificially clamped at zero using an experimental apparatus that places the target image on the fovea [Barnes et.al., 1995, Morris and Lisberger, 1987, Stone and Lisberger, 1990]. Despite zero retinal error, the eye continues to track the target, suggesting that extraretinal signals drive the pursuit system.

This paper is a companion to [Broucke, 2019]. That paper presents a proof of correctness, a discussion of the control architecture and corresponding neural circuit, and simulations based primarily on neurological and lesion experiments. This paper presents a complementary set of simulations focusing primarily on behavioral experiments.

2. ERROR MODEL

We consider only the horizontal motion of one eye. The eyeball is modeled as a sphere suspended in fluid and subject to viscous drag, elastic restoring forces, and the pulling of two muscles [Robinson, 1981, Sylvester and Cullen, 1999]. A reasonable appproximation of the dynamics is obtained by assuming that the inertia of the eyeball is insignificant. Letting x be the horizontal eye angle and u be the net torque imparted by the two muscles, we obtain the standard first order model for the *oculomotor plant*

$$\dot{x} = -K_x x + u\,. \tag{1}$$

The parameter $K_x > 0$ is constant (or very slowly varying) such that the time constant of the eye is $\tau_x := 1/K_x \simeq 0.2$s [Robinson, 1981].

⋆ Supported by the Natural Sciences and Engineering Research Council of Canada (NSERC).

It has been shown experimentally that proprioception from the eye muscles plays a negligible role in eye movement [Guthrie et.al., 1983] and that eye position information is available in the brainstem via a *brainstem neural integrator* modeled as a leaky integrator [Skavenski and Robinson, 1973]. In control theoretic terms, the neural integrator is an observer

$$\dot{\hat{x}} = -\widehat{K}_x \hat{x} + u \,, \tag{2}$$

where $\hat{x}$ is an estimate of the eye position and $\widehat{K}_x \simeq K_x$ [Skavenski and Robinson, 1973] (henceforth we drop the hat). Aside from a momentary perturbation (a push on the eyeball), $\hat{x}(t)$ well approximates $x(t)$.

Consider a reference signal r representing the angle of a target moving in the horizontal plane. The reference signal is regarded as a persistent unmeasurable disturbance acting on the oculomotor system. Let x_h and $\dot{x}_h$ be the horizontal head angular position and angular velocity, respectively, with respect to an inertial reference frame. The *retinal error* is defined to be

$$e := \alpha_e (r - x_h - x) \,. \tag{3}$$

Notice that $r - x_h - x$ is the target angle r relative to the *gaze angle* $x_h + x$. For sufficiently distant targets, this relative angle is proportional (through a scale factor $\alpha_e \in \mathbb{R}$) to a linear displacement on the retina from the fovea to the target. Since the goal of the slow eye movement systems is to drive e to zero, for the purposes of the present paper we set $\alpha_e = 1$, since for $\alpha_e \neq 1$ we can always redefine the error to be $e' = e/\alpha_e$.

We assume that the control input u takes the form

$$u = u_b + u_c \,,$$

where the brainstem component u_b is generated through a brainstem-only pathway, while the cerebellar component u_c is generated by a side pathway through the cerebellum. The vestibular system provides a measurement of the head angular velocity $\dot{x}_h$ to the brainstem but not directly to the cerebellum [Gerrits, 1989, Lisberger, 2009], and it does not provide the head position x_h [Robinson, 1981]. Finally, we assume that the cerebellum receives a measurement of the retinal error e (or a scaled version of it) [Basso et.al., 2000, Glasauer, 2003, Krauzlis, 1997].

Remark 1. Each of the eye movement systems has driving signals, signals required for computation of ongoing eye movement. Head velocity is a driving signal for the vestibulo-ocular reflex (VOR). The *retinal slip velocity*, the derivative of retinal error, is often assumed to be the driving signal for the smooth pursuit system. On the other hand, it is known that in primates, the slow eye movement systems share the same neural pathways in the brainstem and cerebellum, so it is plausible these systems share certain driving signals. In this paper we assume that the common visual driving signal shared by the slow eye movement systems is the retinal error; experimental evidence supporting our assumption is reported in [Jones and Mandl, 1979, Pola and Wyatt, 1980, Mandl et.al., 1981, Wyatt and Pola, 1983, Berthoz, 1988, Shelhamer et.al., 1994, 1995, Zhou et.al., 2001, Eggers et.al., 2003, Blohm et.al., 2005]. An fruitful investigation would be to modify our model such that the retinal slip velocity is the driving signal. ◁

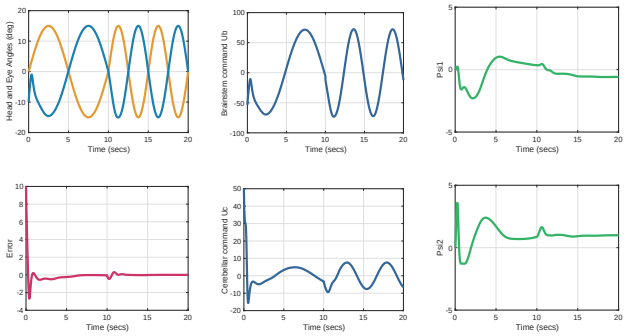

Fig. 1. VOR with a sinusoidal head rotation. The top left figure shows the head (yellow) and eye (blue) angles. The bottom left is the retinal error (red). The middle figures are u_b and u_c, and the right figures are the parameter estimates $\hat{\Psi}_1$ and $\hat{\Psi}_2$.

Define $\alpha_x \in \mathbb{R}$ and $\alpha_h \in \mathbb{R}$ to be constant (or very slowly varying) parameters, and define the brainstem-only pathway of the control input to be

$$u_b = \alpha_x \hat{x} - \alpha_h \dot{x}_h \,. \tag{4}$$

The role of u_b is to suppress a portion of the head velocity disturbance in the error dynamics and to approximately cancel the drift term in the oculomotor plant dynamics.

Finally, assuming that $\hat{x}(t) \simeq x(t)$ for $t \geq 0$, we obtain the *open-loop error model*

$$\dot{e} = -\tilde{K}_x e - u_c + \dot{r} + \tilde{K}_x r - (1 - \alpha_h)\dot{x}_h - \tilde{K}_x x_h \,, \tag{5}$$

where $\tilde{K}_x := K_x - \alpha_x$.

3. MODEL OF THE OCULOMOTOR SYSTEM

As mentioned, the premise of our modeling approach is to treat the cerebellum as an adaptive internal model [Nikiforov, 1996, 1997, 1998, Serrani and Isidori, 2000, Serrani et.al., 2001, Marino and Tomei, 2011, 2013]. First, we assume the reference signal r as well as the head position x_h can be modeled as the outputs of an unknown linear exosystem. Let $\eta \in \mathbb{R}^q$ be the exosystem state and define the exosystem

$$\dot{\eta} = S\eta \,, \quad r = D_1 \eta \,, \quad x_h = D_2 \eta \,, \tag{6}$$

where $S \in \mathbb{R}^{q \times q}$, $D_1 \in \mathbb{R}^{1 \times q}$, and $D_2 \in \mathbb{R}^{1 \times q}$. Then (5) takes the form

$$\dot{e} = -\tilde{K}_x e - u_c + E\eta \tag{7}$$

where $E := D_1 S + \tilde{K}_x D_1 - (1 - \alpha_h) D_2 S - \tilde{K}_x D_2 \in \mathbb{R}^{1 \times q}$. Using the technique in [Nikiforov, 1998], the exosystem can be transformed to

$$\dot{w} = (F + G\Psi) w \,, \tag{8}$$

where (F, G) is a controllable pair, F is Hurwitz, and $E\eta = \Psi w$. Thus, (7) becomes

$$\dot{e} = -\tilde{K}_x e - u_c + \Psi w \,. \tag{9}$$

The parameters $(\tilde{K}_x, \Psi^{\mathrm{T}}) \in \mathbb{R}^{q+1}$ capture all unknown model and disturbance parameters.

The *adaptive internal model* consists of an internal model of the disturbances acting on the oculomotor system combined with a parameter estimation process to recover the unknown parameters. Let $\hat{w}$ and $\hat{\Psi}$ be estimates of w and Ψ, respectively. The controller is

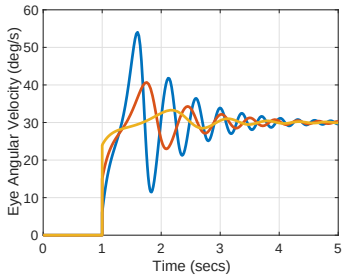

Fig. 2. VOR with a step input in head velocity for the values $\alpha_h = 0.3, 0.5, 0.8$ (blue, red, yellow). The size of the overshoot in the eye velocity is inversely proportional to the value of α_h.

$$\dot{\hat{w}} = F\hat{w} + Gu_c \tag{10}$$

$$u_c = u_{imp} + u_s\,. \tag{11}$$

The controller u_{imp} is selected to satisfy the internal model principle: $u_{imp} = \hat{\Psi}\hat{w}$. The adaptation law for the parameter estimates is $\dot{\hat{\Psi}} = e\hat{w}^{\mathrm{T}}$. The controller u_s is selected to make the closed-loop system asymptotically stable. We choose $u_s = K_e e$, with $K_e > 0$ sufficiently large (see Serrani and Isidori [2000], Serrani et.al. [2001]).

The overall model of the oculomotor system is:

$$\dot{x} = -K_x x + u \tag{12a}$$

$$\dot{\hat{x}} = -K_x \hat{x} + u \tag{12b}$$

$$\dot{\hat{w}} = F\hat{w} + Gu_c \tag{12c}$$

$$\dot{\hat{\Psi}} = e\hat{w}^{\mathrm{T}} \tag{12d}$$

$$u_b = \alpha_x \hat{x} - \alpha_h \dot{x}_h \tag{12e}$$

$$u_c = \hat{\Psi}\hat{w} + K_e e \tag{12f}$$

$$u = u_b + u_c\,. \tag{12g}$$

In the following sections this model will be validated under a number of experimental scenarios. The nominal parameter values for the simulations are: $q = 2$, $K_x = 5$, $\alpha_x = 0.95K_x$, $\alpha_h = 0.65$, $K_e = 5$, $\lambda_1 = 1$, and $\lambda_2 = 1$.

4. VESTIBULO-OCULAR REFLEX

The purpose of the vestibulo-ocular reflex (VOR) is to keep the gaze (sum of eye and head angles) stationary when the head is moving. A standard VOR experiment is to apply an involuntary sinusoidal head rotation: $x_h(t) = a_h \sin(\beta_h t)$, where $a_h, \beta_h > 0$. In order that vision not be smeared out, the eye must move opposite to the head rotation. The brainstem already provides part of this disturbance suppression through the term $-\alpha_h \dot{x}_h$. In our model the cerebellum supplies the remaining disturbance suppression required.

Figure 1 shows simulation results for the values $a_h = 15$, $\beta_h = 0.1$Hz for $t \in [0, 10]$, and $\beta_h = 0.2$Hz for $t \in [10, 20]$. The initial condition on all states is zero except the eye angle, which starts at $x(0) = -10°$. We also plot the retinal error, the cerebellar and brainstem components of the control input, and the parameter estimates $\hat{\Psi}_1$ and $\hat{\Psi}_2$. As expected, the eye moves opposite to the head rotation, and it adapts to the frequency of the sinusoidal disturbance.

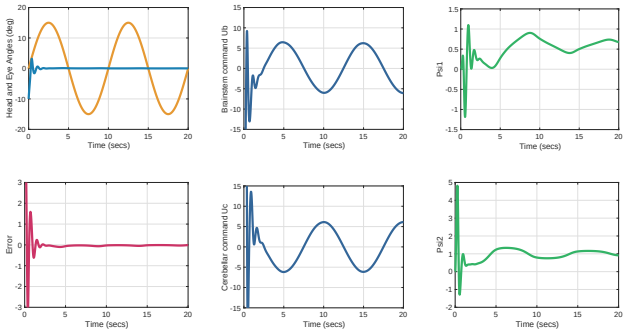

Fig. 3. VOR cancellation. The signals are the same as in Figure 1. Despite the fact that the eye is stationary, u_b and u_c are not zero.

Transients of the VOR in monkeys were investigated in [Lisberger and Pavelko, 1986]. It was discovered that the overshoot in the eye velocity to a sudden rotation of the head was larger when the *VOR gain* (our parameter α_h) is smaller. In the experiment, a light spot at $r = 0$ on which the monkey fixates (in another otherwise dark room) is strobed. Here we assume the subject attempts to continuously fixate the eyes on a target at $r = 0$, even when the light spot is extinguished. The head position is a ramp function: $x_h(t) = 0$ for $t \in [0, 1]$ and $x_h(t) = -30t$ for $t \in [1, 5]$, resulting in a head angular velocity of -30°/s. Figure 2 illustrates that our model recovers the behavior in [Lisberger and Pavelko, 1986]. The blue curve is the eye angular velocity for $\alpha_h = 0.3$, red is with $\alpha_h = 0.5$, and yellow is with $\alpha_h = 0.8$. We see clearly that smaller VOR gains result in larger overshoots.

In an experiment called *VOR cancellation*, the head is rotated involuntarily while the eyes must track a head-fixed target. Suppose the head angle is $x_h(t) = a_h \sin(\beta_h t)$ with $a_h, \beta_h > 0$, and the target angle is $r(t) = x_h(t)$. Then the error is given by $e = -x$. The role of u_{imp} in this case is to cancel the disturbance $\alpha_h \dot{x}_h$ introduced by the brainstem component u_b. Figure 3 illustrates the results for VOR cancellation using our model. Particularly, we note that the response amplitude of the brainstem component is not reduced during VOR cancellation, as experimentally confirmed in [Buettner and Buttner, 1979, Keller, 1975].

Next, we consider what happens when the head is rotated in darkness. In this case the cerebellum is relatively inactive due to a lack of visual input [Lisberger, 2015]. As such, we assume in darkness $u_c = 0$, so the eye dynamics evolve according to a brainstem-only control input. Assuming that $x(t) \simeq \hat{x}(t)$, we have

$$\dot{x} = -\tilde{K}_x x - \alpha_h \dot{x}_h\,. \tag{13}$$

Assuming $\tilde{K}_x > 0$, the steady-state response $x_{ss}(t)$ has the form

$$x_{ss}(t) = -\alpha_h a_h \frac{\beta_h^2}{\tilde{K}_x^2 + \beta_h^2}\big(\sin(\beta_h t + \varphi)\big)\,,$$

where φ is a phase shift. Generally $\tilde{K}_x^2/\beta_h^2 \simeq 0$, so

$$x_{ss}(t) \simeq -\alpha_h a_h \sin(\beta_h t) = -\alpha_h x_h(t)\,.$$

That is, the eye moves relative to the head with a scale factor of -α_h. The parameter α_h is called the *VOR gain*

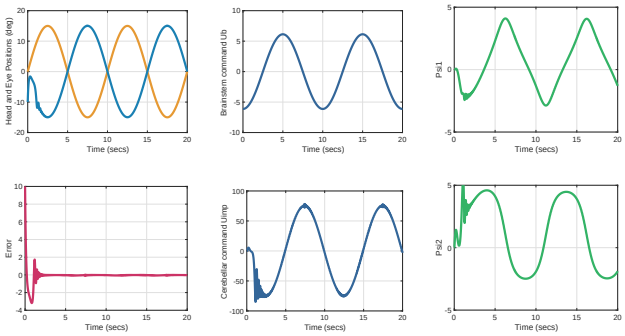

Fig. 4. VOR in the light with the neural integrator disabled. The signals are the same as in Figure 1.

since it well approximates the ratio of head velocity to eye velocity measured in darkness.

A study of the effects of disabling the neural integrator on the VOR, OKR, and smooth pursuit in monkeys appeared in [Kaneko, 1999]. They found these systems are minimally affected after a recovery period. In our model, disabling the neural integrator corresponds to removing the observer (12b). This means the brainstem component of the control input no longer includes the estimate $-\alpha_x \hat{x}$. Our model predicts that in the light, the cerebellum will compensate for the additional disturbance, such that the VOR is only mildly affected, as reported in Kaneko [1999]. Figure 4 shows the behavior of the VOR in the light with the neural integrator disabled, $x_h(t) = a_h \sin(\beta_h t)$, $a_h = 15$, and $\beta_h = 0.1$Hz for $t \in [0, 20]$. We observe the eye moves opposite to the head rotation, as expected.

5. OPTOKINETIC REFLEX

The purpose of the *optokinetic reflex* (OKR) is to reduce image motion across the retina when a large object or the entire visual surround is moving. This system operates in tandem with the VOR. Consider the case of the visual surround rotating sinusoidally, $r_{vs}(t) = -a_v \sin(\beta_v t)$, for example by using an optical drum [Baarsma and Collewijn, 1974]. The head may be stationary, moving with the visual surround, or moving independently but involutarily. The eyes may be fixating on a stationary target, a head-fixed target, a drum-fixed target, or a target moving within the moving visual field.

One way to interpret the OKR is that the motion of the visual surround induces in the subject a perception of a stationary background, with the head and target moving with respect to (w.r.t.) this stationary background. If $r(t)$ and $x_h(t)$ are the target and head angles w.r.t. a fixed inertial frame, then the perceived head and target motion w.r.t. the visual surround are given by $r_p(t) = r(t) - r_{vs}(t)$ and $x_{hp}(t) = x_h(t) - r_{vs}(t)$. The perceived error is given by $e_p = r_p - x_{hp} - x = r - x_h - x$. Mathematically speaking, the OKR is the same as the VOR with a fixed visual surround.

For example, in many experiments with the OKR, the eyes must track a drum-fixed light slit with the head stationary and the optical drum rotating sinusoidally. In this case the error is $e = r - x$, where $r(t) = a_h \sin(\beta_h t)$. This situation is the same as smooth pursuit, to be discussed below. In an experiment called *OKR cancellation*, a light spot at $r = 0$ is placed in front of a moving striped optical drum. In this

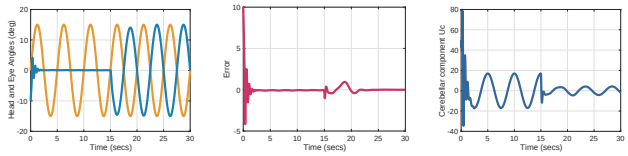

Fig. 5. Visuo-vestibular conflict in the OKR and its effect on the depth of modulation of the cerebellar component u_c. From left to right, the head (yellow) and eye (blue) angles, the retinal error e, and the cerebellar component u_c. Despite the fact that the eye is nearly stationary during $t \in [0, 15]$, the amplitude of u_c is larger than when the optokinetic drum is rotating during $t \in [15, 30]$.

case, the pursuit system appears to override the OKR, as the eyes fixate on the fixed light spot, and the error is $e = -x$. If there is no head rotation, then this situation is the same as gaze fixation, discussed in the next section.

In an experiment called *visual-vestibular conflict* the head and the optokinetic drum are mechanically coupled so that they rotate together, and the eyes must track a light strip on the drum [Baarsma and Collewijn, 1974]. Therefore, we have $r(t) = x_h(t) = a_h \sin(\beta_h t)$, so $e = -x$. Mathematically, this situation is no different than VOR cancellation. It has been reported that under such stimulation, the modulation of the firing rate of the cerebellum is larger than when the drum is not rotated [Waespe and Henn, 1978]; that is, when $r(t) = 0$, $x_h(t) = a_h \sin(\beta_h t)$, and $e = -x_h - x$. In the context of our model, this finding makes sense. In the first case, the role of u_{imp} is to cancel the term $\alpha_h \dot{x}_h$. In the second case, the role of u_{imp} is to cancel the term $-(1 - \alpha_h)\dot{x}_h - \tilde{K}_x x_h$. Assuming that α_h is not close to 0.5 and that $\tilde{K}_x$ is close to zero, the amplitude of the disturbance $\alpha_h \dot{x}_h$ is larger than the amplitude of the disturbance $-(1-\alpha_h)\dot{x}_h - \tilde{K}_x x_h$. Figure 5 illustrates this comparison for values $\alpha_h = 0.9$; $a_h = 15$; $\beta_h = 0.2$Hz; $r = x_h = a_h \sin(\beta_h t)$ for $t \in [0, 15]$; and $r = 0$, $x_h = a_h \sin(\beta_h t)$ for $t \in [15, 30]$. We observe in the right figure that the amplitude of u_c is larger when the drum is rotated during the interval $t \in [0, 15]$ than when it is stationary during $t \in [15, 30]$.

6. GAZE FIXATION

The purpose of the *gaze fixation system* is to stabilize the gaze on a stationary object. Consider a target with an angle $r \neq 0$ and the head angle $x_h = 0$. The error is given by $e = r - x$. Assuming that $\hat{x}(t) \simeq x(t)$, the error dynamics (9) take the form

$$\dot{e} = -\tilde{K}_x e - u_c + \tilde{K}_x r \,. \tag{14}$$

We can see that the role of u_{imp} is to estimate the disturbance $\tilde{K}_x r$. Figure 6 shows the behavior when $\alpha_h = 0.65$ and the target angle is: $r(t) = 5°$ for $t \in [0, 15]$; $r(t) = 10°$ for $t \in [15, 30]$, and $r(t) = 15°$ for $t \in [15, 45]$. We observe that the cerebellar component of the control input is proportional to the eye angle, a behavior observed experimentally in many studies [Noda and Suzuki, 1979]. It arises in our model because u_{imp} must cancel a disturbance $\tilde{K}_x r$ which is proportional to the target position.

Further evidence that $\tilde{K}_x \neq 0$ comes from studies in which the cerebellum is disabled, either through ablation

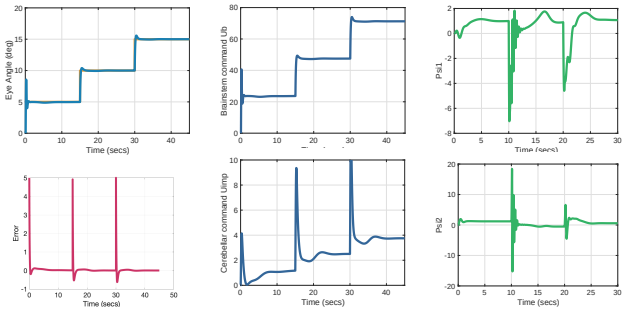

Fig. 6. Gaze fixation. The signals are the same as in Figure 1.

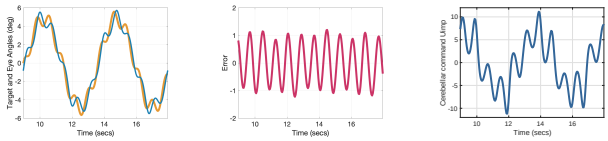

Fig. 7. Smooth pursuit of a sum of two sinusoids. From left to right, the target angle (yellow) and eye angle (light blue), the error e (red), and the cerebellar output u_{imp} (blue).

or disease. It is often observed in this case that the eye has a slow drift back to the central position $x = 0$ [Carpenter, 1972, Noda and Suzuki, 1979, Skavenski and Robinson, 1973]. Mathematically, suppose that $x_h = 0$ and $u_c = 0$. Then $u = u_b = \alpha_x \hat{x}$, and assuming $\hat{x}(t) \simeq x(t)$, the eye position evolves according to the dynamics $\dot{x} = -\tilde{K}_x x$. That is, the eye drifts back to center at an exponential rate determined by $\tilde{K}_x$.

7. SMOOTH PURSUIT

The purpose of the smooth pursuit system is to keep a moving object centered on the fovea. As before, let $r(t)$ be the target angle and $x_h(t)$ the head angle. Assuming that $\hat{x}(t) \simeq x(t)$, the error dynamics take the general form in (5), and the role of u_{imp} is to estimate the disturbance $\dot{r} + \tilde{K}_x r - (1 - \alpha_h)\dot{x}_h - \tilde{K}_x x_h$.

The perfect tracking capability of the smooth pursuit system has been well documented over the years; a small sampling includes [Bahill and McDonald, 1983, Collewijn and Tamminga, 1984, Deno et.al, 1995]. This tracking capability improves as the targe motion becomes more predictable [Bahill, 1983].

Figure 7 depicts the behavior of our model for smooth pursuit of a target $r(t) = a_1 \sin(2\pi\beta_1 t) + a_2 \sin(2\pi\beta_2 t)$, with $a_1 = 4.85$, $\beta_1 = 0.22$Hz, $a_2 = 0.853$ and $\beta_2 = 1.25$Hz. The time interval $t \in [9, 18]$ was chosen to match the data in Figure 1 of Barnes et.al. [1987]. This simulated behavior reproduces what is observed in experiments; namely, that while humans are not capable of perfect tracking of a sum of two or more sinusoids, nevertheless the smooth pursuit system performs reasonably well. The non-zero error displayed in the center of Figure 7 is corroborated by experimental findings in Barnes et.al. [1987]. Figure 8 depicts the behavior of our model for smooth pursuit of a target $r(t) = a_1 \sin(2\pi\beta_1 t) + \cdots + a_4 \sin(2\pi\beta_4 t)$, with $a_1 = 6.94$, $\beta_1 = 0.214$Hz, $a_2 = 2.86$, $\beta_2 = 0.519$Hz, $a_3 = 2.11$, $\beta_3 = 0.702$Hz, $a_4 = 1.57$, and $\beta_4 = 0.946$Hz. The results

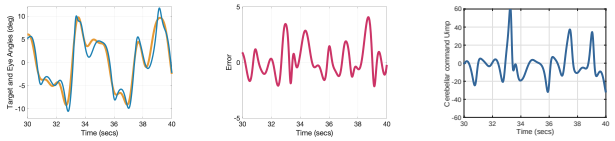

Fig. 8. Smooth pursuit of a sum of four sinusoids. From left to right, the target angle (yellow) and eye angle (light blue), the error e (red), and the cerebellar output u_{imp} (blue).

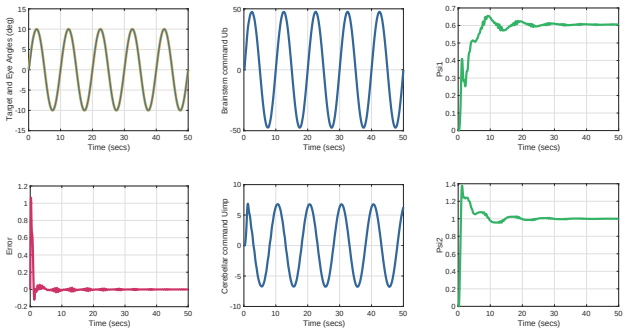

Fig. 9. Smooth pursuit of a sinusoidal target with a time delay of 107ms in the retinal error signal. The signals are the same as in Figure 1.

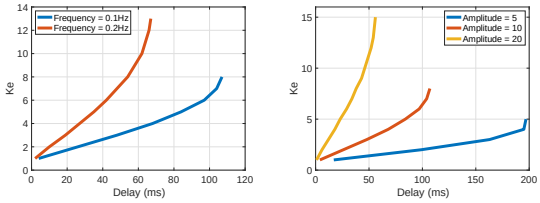

Fig. 10. Maximum time delay as a function of K_e.

are comparable to those obtained experimentally as shown in Figure 2 of Collewijn and Tamminga [1984].

It is known that the processing delay for the retinal error to arrive at the cerebellum is on the order of 100ms. Nevertheless, the smooth pursuit system achieves nearly perfect tracking capability; its ability to do so in the face of this delay has been interpreted as a predictive capabability Deno et.al [1995]. Our model does not impart any prediction to the smooth pursuit system, but the presence of the adaptive internal model aids in overcoming delays. Figure 9 depicts the behavior when tracking a sinusoidal target $r(t) = a \sin(2\pi\beta t)$ with $a = 10$ and $\beta = 0.1$Hz. The error e has been replaced by $e(t - \tau)$ in (12d) and (12f), with a time delay of $\tau = 107$ms. The other parameter values are the same as before but we set $K_e = 8$ for closed-loop stability. We observe there is little degradation in the system's tracking capability.

The choice of K_e to achieve closed-loop stability is tied to the time delay and the magnitude of the reference $r(t)$. Figure 10 depicts the largest delay attained with the smallest K_e for varying frequencies and amplitudes of reference signals of the form $r(t) = a \sin(2\pi\beta t)$. With $a = 10$ and $\beta = \{0.1, 0.2\}$Hz, delays of 107ms and 67ms were achieved with K_e equal to 8 and 13, respectively. Holding $\beta = 0.1$Hz but with $a = \{5, 10, 20\}$, the model overcomes delays of 197ms, 107ms, and 56ms with K_e equal to 5, 8 and 15, respectively.

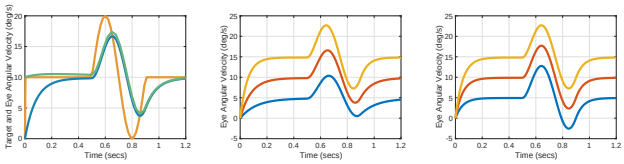

Fig. 11. Smooth pursuit of a ramp target with a sinusoidal perturbation. The left figures shows the target velocity (yellow) and eye velocity (light blue). The middle figure shows the eye velocity as a function of the parameters $(v, K_e) = (5, 8), (10, 8), (15, 8)$.

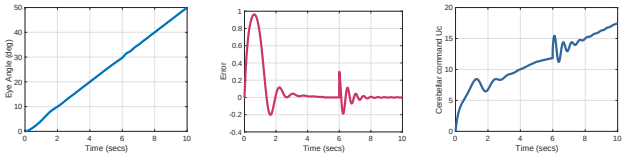

Fig. 12. Smooth pursuit with an error clamp during $t \in [5, 6]$s. From left to right, the eye angle (blue), the retinal error e, and the cerebellar component u_c. The eye continues to move and the cerebellum remains active during the error clamp.

A number of experimental studies have shown that the smooth pursuit system is capable of a mechanism of gain control Nuding et.al. [2008, 2009], Lisberger [2010], Lee et.al. [2013], Ono [2015], Brostek et.al. [2017]. This mechanism, first proposed in Robinson [1965], is thought to regulate an internal gain parameter in which higher target velocities yield higher gains. The mechanism appears to be dedicated to the smooth pursuit system, as several studies have shown that gain control is less prominent in the gaze fixation system Lee et.al. [2013].

Gain control in the smooth pursuit system is related to the gain K_e in our model. A Lyapunov-based argument implies that this parameter must be increased as a function of the magnitude and frequency of disturbances in order to maintain closed-loop stability Serrani and Isidori [2000]. Gain control experiments suggest that this parameter may not be constant, but rather may be a function of either the retinal error e or the retinal slip velocity $\dot{e}$, thereby yielding a nonlinear stabilization mechanism. Here we investigate the extent to which varying K_e as a function of the size of perturbations can explain the experimental data.

We consider an experiment in Ono [2015] in which a brief sinusoidal perturbation is introduced during ongoing pursuit of a ramp target. The target velocity is $\dot{r}(t) = v°/s$ for $t \in [0, 0.5]$s; $\dot{r}(t) = v + v\sin(2\pi\beta)°/s$ for $t \in [0.5, 0.9]$; and $r(t) = v°/s$ for $t \in [0.9, 1.2]$. First we set $v = 10$, $K_e = 12$, and $\alpha_1 = \alpha_2 = 10$. The left Figure 11 depicts the target (yellow) and eye (blue) velocities. The result closely matches the eye velocity obtained experimentally in Figure 2A of Ono [2015]. The parameters α_1 and α_2 have been set to increase the adaptation rate of the adaptive internal model so that by the time the perturbation occurs, the internal model is already tuned to a ramp reference signal. Based on recordings in the visual cortex, Ono observed that visual related neurons showed a significant modulation in firing rate associated with the perturbation. In contrast, pursuit related neurons carrying an extraretinal signal did not show a corresponding modulation in firing rate despite a prominent change in eye motion. In our model, the visual related neurons would carry the visual signal $K_e e$, so the experimental observations would suggest that the eye velocity during perturbation is mainly driven by the signal $K_e e$. To test this hypothesis, we set $\alpha_1 = \alpha_2 = 1$, $\hat{\Psi}_1(0) = 1$, $\hat{\Psi}_2(0) = 1$, $w_1(0) = 0$ and $w_2(0) = 10$, and we disabled the parameter adaptation in (12d). Effectively, the adaptive internal model is already adapted to a ramp input prior to the experiment (as may happen for a subject performing repeated experiments with ramp inputs). The result is depicted in the green curve on the left of Figure 11, showing the eye velocity for the pre-adapted internal model. Since it closely matches the blue curve during the perturbation, we can conclude that error feedback does indeed dominate the change in eye velocity during the perturbation.

Next, to expose the gain control mechanism we consider the same target motion with three baseline velocities $v = 5, 10, 15°/s$ and three corresponding gains $K_e = 8, 10, 15$. The eye velocity is shown in the middle of Figure 11. These results correspond almost exactly with the experimental results obtained in Figure 3B of Ono [2015]. If instead we fix the gain $K_e = 12$ for all three baseline velocities, we obtain the eye velocities on the right of Figure 11. This response no longer matches the experimental results in two aspects: the distinctive variation in rise time and the distinctive variation in the size of the response to the perturbation are both absent. Based on this first look, the gain control mechanism of the smooth pursuit system may be modeled by allowing K_e to be a function of retinal signals.

Lastly, we consider the *error clamp* experiment which explores the role of the error signal using a technique called *retinal stabilization* [Barnes et.al., 1995, Morris and Lisberger, 1987, Stone and Lisberger, 1990]. A monkey is trained to track a visual target moving at constant speed. After reaching steady-state, the retinal error is optically clamped at zero using an experimental apparatus that places the target image on the fovea. In experiments it is observed that the eye continues to track the target for some time after. Figure 12 depicts the error clamp behavior with our model, showing that the eye continues to track the target despite the error being clamped at $e \equiv 0$ during the time interval $t \in [5, 6]$.

8. CONCLUSION

We have proposed a control-theoretic model of the oculomotor system, particularly the slow eye movement systems: the VOR, OKR, gaze fixation, and smooth pursuit. Our key insight is to exploit developments in control theory on adaptive internal models [Nikiforov, 1996, 1997, 1998, Serrani and Isidori, 2000, Serrani et.al., 2001, Marino and Tomei, 2011, 2013]. Our model recovers results from a number of experiments. Additionally, we make a proposal about a role of the cerebellum: *to embody adaptive internal models of all persistent, exogenous reference and disturbance signals acting on the body.* Our forthcoming work will apply our cerebellar model to the saccadic system for fast eye movements, as well as to other human motor control systems. **Acknowledgements:** The author thanks Erin Battle, Heyang Yan, and Yuyao Wei for performing some of the simulations.

REFERENCES

E. Baarsma and H. Collewijn. Vestibulo-ocular and optokinetic reactions to rotation and their interaction in the rabbit. *J. Physiology.* Vol. 238, pp. 603–625, 1974.

A.T. Bahill and J. McDonald. Model emulates human smooth pursuit system producing zero-latency target tracking. *Biological Cybernetics.* No. 48, pp. 213-222, 1983.

A.T. Bahill and J. McDonald. Smooth pursuit eye movements in response to predictable target motions. *Vision Research.* Vo. 23, No. 12, pp. 1573–1583, 1983.

G.R. Barnes, S.F. Donnelly, and R.D. Eason. Predictive velocity estimation in the pursuit reflex response to pseudo-random and step displacement stimuli iin man. *J. Physiology.* Vol. 389, pp. 111-136, 1987.

G. Barnes, S. Goodbody, and S. Collins. Volitional control of anticipatory ocular pursuit responses under stabilized image conditions in humans. *Experimental Brain Research.* No. 106, pp. 301317, 1995.

M. Basso, R. Krauzlis, and R. Wurtz. Activation and inactivation of rostral superior colliculus neurons during smooth-pursuit eye movements in monkeys. *Journal of Neurophysiology.* No. 84, pp. 892-908, 2000.

A. Berthoz. The role of gaze in compensation of vestibular dysfunction: the gaze substitution hypothesis. *Progress Brain Research.* No, 76, pp. 411-420, 1988.

G. Blohm, M. Missal, and P. Lefevre. Direct evidence for a position input to the smooth pursuit system. *Journal of Neurophysiology.* Vol. 94, pp. 712-721, 2005.

L. Brostek, T. Eggert, and S. Glasauer. Gain control in predictive smooth pursuit eye movements: evidence for an acceleration-based predictive mechanism. *eNeuro.* Vol. 4, No. 3, May/June 2017.

M. Broucke. Adaptive internal model theory of the oculomotor system and the cerebellum. *IEEE Transactions on Automatic Control.* Submitted January, 2019.

U. Buettner and U. Buttner. Vestibular nuclei activity in the alert monkey during suppression of vestibular and optokinetic nystagmus. *Exp. Brain Res.* No. 37, pp. 581-593, 1979.

R.H.S. Carpenter. Cerebellectomy and the transfer function of the vestibulo-ocular reflex in the decerebrate cat. *Proc. Royal Society of London. Series B, Biological Sciences.* Vol. 181, No. 1065, pp. 353–374, July 1972.

N. Cerminara, R. Apps, and D. Marple-Horvat. An internal model of a moving visual target in the lateral cerebellum. *J. Physiology.* vol. 587, no. 2, pp. 429-442, 2009

M. Churchland, I. Chou, and S. Lisberger. Evidence for object permanence in the smooth-pursuit eye movements of monkeys. *J. Neurophysiology.* No. 90, pp. 2205-2218, 2003.

H. Collewijn and E. Tamminga. Human smooth and saccadic eye movements during voluntary pursuit of different target motions on different backgrounds. *J. Physiology.* vol. 351, pp. 217-250, 1984.

P. Dean and J. Porrill. Adaptive-filter models of the cerebellum: computational analysis. *Cerebellum.* No. 7, pp. 567-571, 2008.

D.C. Deno, W.F. Crandall, K. Sherman, E. Keller. Characterization of prediction in the primate visual smooth pursuit system. *BioSystems.* vol. 34, pp. 107–128, 1995.

S. Eggers, N. de Pennington, M. Walker, M. Shelhamer, and D. Zee. Short-term adaptation of the VOR: non-retinal-slip error signals and saccade substitution. *Ann. N.Y. Academy of Sciences.* No. 1004, pp. 94-110, 2003.

B.A. Francis and W.M. Wonham. The internal model principle for linear multivariable regulators. *Applied Mathematics and Optimization.* Vol. 2, No. 2, 1975.

B.A. Francis and W.M. Wonham. The internal model principle of control theory. *Automatica.* Vol. 12, pp. 457–465, 1976.

N.M. Gerrits, A.H. Epema, A.van Linge, and E. Dalm. The primary vestibulocerebellar projection in the rabbit: absence of primary afferents in the flocculus. *Neuroscience Letters.* Vol. 105, pp. 27-33, 1989.

S. Glasauer. Cerebellar contribution to saccades and gaze holding. *Annals New York Academy of Sciences.* pp. 206-209, 2003.

H. Gomi and M. Kawato. Adaptive feedback control models of the vestibulocerebellum and spinocerebellum. *Biological Cybernetics.* Vol. 68, pp. 105-114, 1992.

B. Guthrie, J. Porter, and D. Sparks. Corollary discharge provides accurate eye position information to the oculomotor system. *Science.* Vol. 221, pp. 1193-1195, September 1983.

C. Kaneko. Eye movement deficits following ibotenic acid lesions of the nucleus prepositus hypoglossi in monkeys. *J. Neurophysiology.* Vol. 81, No. 2, pp. 668-681, February 1999.

M. Kawato and H. Gomi. A computational model of four regions of the cerebellum based on feedback-error learning. *Biological Cybernetics.* Vol. 68, pp. 95-103, 1992.

E. Keller and P. Daniels. Oculomotor related interaction of vestibular nucleus cells in alert monkey. *Exp. Neurology.* No. 46, pp. 187-198, 1975.

R. Krauzlis, M. Basso, and R. Wurtz. Shared motor error for multiple eye movements. *Science.* No. 276, pp. 16931695, 1997.

R. Krauzlis and F. Miles. Transitions between pursuit eye movements and fixation in the monkey: dependence on context. *J. Neurophysiology.* No. 76, pp 1622-1638, 1996.

J. Lee, J. Yang, and S. Lisberger. Control of the Gain of VisualMotor Transmission Occurs in Visual Coordinates for Smooth Pursuit Eye Movements. *J. Neuroscience.* Vol. 33, no. 22, pp. 9420 9430, May 2013.

S. Lisberger. Neural basis for motor learning in the vestibuloocular reflex of primates. III. Computational and behavioral analysis of the sites of learning. *J. Neurophysiology.* Vol. 72, No. 2, August 1994.

S. Lisberger. Internal models of eye movement in the floccular complex of the monkey cerebellum. *Neuroscience.* Vol. 162, No. 3, pp. 763–776, September, 2009.

S. Lisberger. Visual guidance of smooth pursuit eye movements: sensation, action, and what happens in between. *Neuron.* No. 66, pp. 477491, 2010.

S. Lisberger. Visual guidance of smooth pursuit eye movements. *Annual Rev. Vis. Sci.* No. 1, pp. 447-468, 2015.

S. Lisberger and A. Fuchs. Role of primate flocculus during rapid behavioral modification of vestibuloocular reflex. I. Purkinje cell activity during visually guided horizontal smooth-pursuit eye movements and passive head rotation. *J. Neurophysiology.* Vol. 41, no. 3, pp. 733–763, May 1978.

S. Lisberger and T. Pavelko. Vestibular signals carried by pathways subserving plasticity of the vestibulo-ocular reflex in monkeys. *Journal of Neuroscience*. No. 6, Vol. 2, pp. 346-354, February 1986.

A. Luebke and D. Robinson. Transition dynamics between pursuit and fixation suggest different systems. *Vision Research*. Vol. 28, No. 8, pp. 941-946, 1988.

G. Mandl, G. Melvill Jones, and M. Cynader. Adaptability of the vestibulo-ocular reflex to vision reversal in strobe reared cats. *Brain Research*. Vol. 209, No. 1, pp. 35-45, 1981.

R. Marino and P. Tomei. An adaptive learning regulator for uncertain minimum phase systems with undermodeled unknown exosystems. *Automatica*. No. 47, pp. 739–747, 2011.

R. Marino and P. Tomei. Disturbance cancellation for linear systems by adaptive internal models. *Automatica*. No. 49, pp. 1494–1500, 2013.

G. Melvill Jones and G. Mandl. Effects of strobe light on adaptation of vestibulo-ocular reflex (VOR) to vision reversal. *Brain Research*. No. 164, pp. 300-303, 1979.

E. Morris and S. Lisberger. Different responses to small visual errors during initiation and maintenance of smooth-pursuit eye movements in monkeys. *J. Neurophysiology*. Vol. 58, no. 6, pp. 1351-1369, 1987.

V. O. Nikiforov. Adaptive servocompensation of input disturbances. em IFAC World Congress. pp. 5114-5119, 1996.

V. O. Nikiforov. Adaptive controller rejecting uncertain deterministic disturbances in SISO systems. *European Control Conference*. pp. 1207-1212, 1997.

V.O. Nikiforov. Adaptive non-linear tracking with complete compensation of unknown disturbances. *European Journal of Control*. Vol. 4, pp. 132–139, 1998.

H. Noda and D. Suzuki. The role of the flocculus of the monkey in fixation and smooth pursuit eye movements. *J Physiology*. No. 294, pp. 335348, 1979.

U. Nuding, S. Ono, M. Mustari, U. Buttner, and S. Glasauer. A theory of the dual pathways for smooth pursuit based on dynamic gain control. *J. Neurophysiology*. No. 99, pp. 2798 2808, 2008.

U. Nuding, R. Kalla, N. Muggleton, U. Buttner, V. Walsh, and S. Glasauer. TMS evidence for smooth pursuit gain control by the frontal eye fields. *Cerebral Cortex*. Vol. 19, pp. 1144 1150, 2009.

S. Ono. The neuronal basis of on-line visual control in smooth pursuit eye movements. *Vision Research*. No. 110, pp. 257-264, 2015.

J. Pola. Models of the saccadic and smooth pursuit systems. In: G. Hung, K. Ciuffreda (eds). *Models of the Visual System*. Springer, 2002.

J. Pola and H. Wyatt. Target position and velocity: the stimulus for smooth pursuit eye movement. *Vision Research*. No. 20, pp. 523-534, 1980.

D. A. Robinson. The mechanics of human smooth pursuit eye movements. *J. Physiology*. No. 180, pp. 569-591, 1965.

J. Porrill, P. Dean, and J. Stone. Recurrent cerebellar architecture solves the motor-error problem. *Proc. Royal Soc. Lond. B*. No. 271, pp. 789-796, 2004.

D.A. Robinson. The use of control systems analysis in the neurophysiology of eye movements. *Ann. Rev. Neuroscience*. No. 4, pp. 463–503, 1981.

D.A. Robinson, J.L. Gordon, and S.E. Gordon. A model of the smooth pursuit eye movement system. *Biological Cybernetics*. No. 55, pp. 43-57, 1986.

A. Serrani and A. Isidori. Semiglobal nonlinear output regulation with adaptive internal model. *IEEE Conference on Decision and Control*. pp. 1649-1654, December, 2000.

A. Serrani, A. Isidori, L. Marconi. Semiglobal nonlinear output regulation with adaptive internal model. *IEEE Transactions on Automatic Control*. Vol. 46, No. 8, pp. 11781194, 2001.

M. Shelhamer, B. Ravina, and P. Kramer. Adaptation of the gain of the angular vestibulo-ocular reflex when retinal slip is zero. *Soc. Neuroscience Abstracts*. No. 21, p. 518, 1995.

M. Shelhamer, C. Tiliket, and D. Roberts, et al. Short-term vestibulo-ocular reflex adaptation in humans II. Error signals. *Experimental Brain Research*. No. 100, pp. 328–336, 1994.

A. Skavenski and D. Robinson. Role of abducens neurons in vestibuloocular reflex. *J. Neurophysiology*. No. 36, pp. 724–738, 1973.

L. Stone and S. Lisberger. Visual responses of Purkinje cells in the cerebellar flocculus during smooth-pursuit eye movements in monkeys I. simple spikes. *Journal of Neurophysiology*. Vol. 63, No. 5, pp. 1241–1261, May 1990.

P. Sylvestre and K. E. Cullen. Quantitative analysis of abducens neuron discharge dynamics during saccadic and slow eye movements. *Journal of Neurophysiology*. Vol. 82, issue 5, pp. 2612–2632, November 1999.

W. Waespe and V. Henn. Conflicting visual-vestibular stimulation and vestibular nucleus activity in alert monkeys. *Experimental Brain Research*. Vol. 33, pp. 203-211, 1978.

D. Wolpert, R.C. Miall, and M. Kawato. Internal models in the cerebellum. *Trends in Cognitive Sciences*. Vol. 2, no. 9, pp. 338–347, September 1998.

H. Wyatt and J. Pola. Smooth pursuit eye movements under open-loop and closed-loop conditions. *Vision Research*. Vol. 23, No. 10, pp. 1121-1131, 1983.

D. Zee, A. Yamazaki, P. Butler, and G. Gucer. Effects of ablation of flocculus and paraflocculus on eye movements in primate. *J. Neurophysiology*. Vol. 46, No. 4, pp. 878–899, October 1981.

X. Zhang and H. Wakamatsu. A unified adaptive oculomotor control model. *International Journal of Adaptive Control and Signal Processing*. No. 15, pp. 697-713, 2001.

W. Zhou, P. Weldon, B Tang and W. King. Retinal slip is not required for rapid adaptation of the translational vestibulo-ocular reflex. *Soc. Neuroscience Abstracts*. No. 27, 2001.